Title: **Structural Health Monitoring in Near-Space Environment, a High Altitude Balloon Test.**

Authors: Andrei Zagrai[1], Benjamin Cooper[1], Jon Schlavin[1], Chris White[1], Seth S. Kessler[2]

Paper to be presented at: ***9**th International Workshop of Structural Health Monitoring*, Sept. 10-12, 2013, Stanford University.

ABSTRACT[1]

The advent of commercial space travel has inspired engineers to rethink design and operation of space transportation systems. Structural health monitoring (SHM) is seen as a promising technology to reduce time to launch and operation costs with simultaneous improvements in the safety of commercial space vehicles. This technology, however, should be validated in realistic environments. In this contribution, exposure of sensors and measurement hardware to the near-space environment was considered and its effect on SHM procedures was investigated. The flight profile of the high-altitude balloon included 1 hour and 36 minutes of accent, 57 minutes of float at 102000 ft and approximately 30 minutes of decent. Three SHM technologies were tested: elastic wave propagation, electro-mechanical impedance, and strain/temperature wireless sensing. The elastic wave propagation experiment consisted of structural sound speed calculation, damage detection, and acoustic emission studies enabled by commercially available hardware. The test was successful, showing variation of sound speed at different stages of the flight and potential to detect structural damage in bolted joint connecting elements of the payload. Acoustic emission activity was also measured. In the second experiment, electro-mechanical impedance of active sensors was measured. However, due to launch delay, only on-the-ground data was collected. The third experiment explored wireless sensing in near-space environment using a commercially available hardware configuration for strain and temperature sensing. Sensor data was collected wirelessly during the high-altitude balloon flight. The study suggests potential of active diagnosis for continuous SHM of space vehicles and indicates specifics of using off-the-shelf sensor solutions in the near-space environment.

1. INTRODUCTION

In recent years, there is an increasing interest in technologies supporting commercial space transportation. SHM is seen as one of technologies enabling rapid launch, monitoring during flight, and post flight structural assessment. Information on vehicle's structural integrity during all stages of the spaceflight is particularly

[1] Department of Mechanical Engineering, New Mexico Institute of Mining and Technology, Socorro, NM 87801, azagrai@nmt.edu, 575-835-5636, Fax 575-835-5209.
[2]Metis Design Corporation, 205 Portland St, Boston, MA 02114.

important for validation of spacecraft operation models and prediction of remaining service life. Such information would be invaluable when stored in a spacecraft flight recorder, a.k.a. “black box”, as it would play critical role in recertification of the space vehicle for the next flight.

A diverse range of sensors is currently flown on space vehicles including temperature, strain, pressure, and even acoustic emission [1,2]. Most of these sensor solutions are highly specialized and feature space-graded hardware units [2,3]. The purpose of this study is to explore use of off-the-shelf sensor solutions and active diagnostics in environments encountered by commercial space vehicles. Certain aspects of such environment may be imitated during high altitude stratospheric balloon flight. Authors are not aware of prior SHM tests conducted during high altitude balloon flights and, therefore, focus of this contribution is to acquaint a reader with preliminary data showing feasibility of active and passive SHM in this environment.

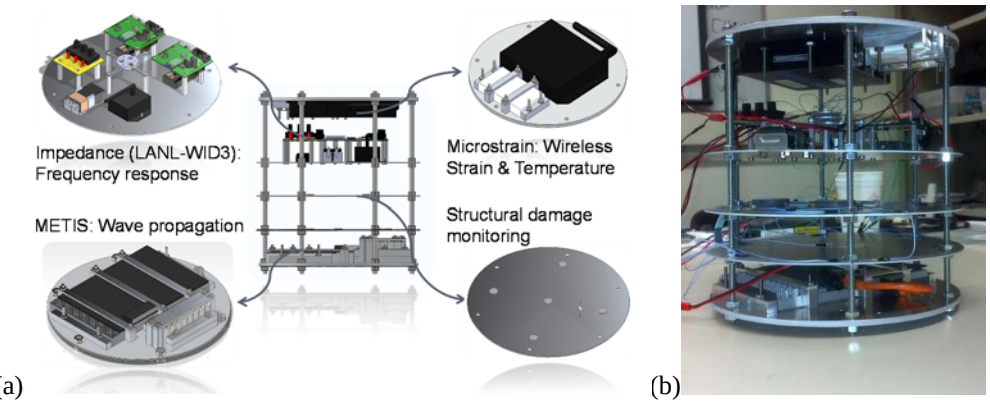

Figure 1 (a) Schematics of stratospheric SHM experiments and (b) photo of actual payload.

2. PAYLOAD DESIGN

The payload was designed as a multilevel structure with threaded pillars connecting and securing five circular plates housing several SHM experiments. Figure 1 provides schematics of the payload and a photograph of its practical implementation.

All horizontal plates in the payload were of the same diameter and were machined from 6061-T6 aluminum. The bottom and top plates were of 1/5" thickness while the three inner plates were only 1/16" thick. The top and bottom plates were thicker because they would be housing the heavier hardware components. The five plates were held together with six 1/4" all-thread 10” (length) rods. Each plate was held in place at particular levels using twelve 1/4" nuts. This method was chosen over a more commonly used stand-offs method to allow for the payload to be modular. If new hardware is added the plates can be moved up or down to easily shift the center of mass and better accommodate diverse hardware configurations. Hardware components were secured on the plates using bolted joints.

SHM experiments flown on the stratospheric balloon flight were battery operated. Capacity of each battery was chosen based on experiment power requirement and data collection rates, which were different for all experiments in the payload. The general design requirement was that each experiment would run for 6 hours. A special breadboard (yellow in Figure 1a) with three electrical switches was constructed to power various experiments in the payload. Successful power transfer

was monitored using light emitting diodes (LED) on the breadboard and on electronic hardware components in each experiment.

3. SHM EXPERIMENTS FLOWN ON A HIGH ALTITUDE BALLOON

The payload contained three hardware modules responsible for six experiments.

3.1 Electro-mechanical impedance measurements

Electro-mechanical impedance measurements were intended for monitoring piezoelectric sensor (PZT) characteristics during flight and elements of structural dynamic testing. The electro-mechanical impedance test hardware – WID3 boards [5] were provided by LANL Engineering Institute [6]. Given the number of channels, memory allocation on the boards, and particularities of software setup, the team intended to collect data during first hour of the flight. Unfortunately, due to unforeseen circumstances, the launch was delayed for one hour while all systems were powered on and, therefore, electro-mechanical impedance data was collected on the ground only. For this reason, no impedance data was collected during flight and reported in this paper.

3.2 Wireless strain and temperature sensing

A wireless sensing experiment was designed to investigate applicability of wireless sensing technology to assess relatively large structures in high altitude (stratosphere) environment. In this flight, large structure included inflated balloon, payload container, and a Mylar ribbon deployed using an automated pulley during float portion of the flight. Figure 2 provides schematics of wireless sensing experiment. Four nodes with autonomous power were deployed: on top of the balloon (apex node), on one of plates in the payload, in the middle and bottom of the ribbon. Sensor communication and data aggregation module was placed inside the payload. It is visible right below top plate in Figure 1b.

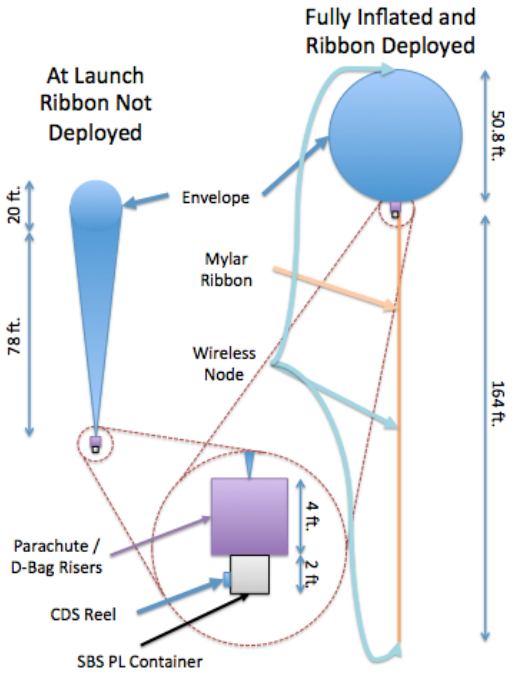

Figure 2 Schematics of wireless sensing experiment.

It is anticipated that space and near space environments will see increasing use of off-the-shelf hardware components to decrease flight and operation costs. Hence, commercially available product, LORD Microstrain wireless system, was selected for this test rather than development of a specialized sensing system. The system consisted of four SG-Link®-LXRS® wireless sensor nodes and WSDA®-1000 data aggregation station. Dimensions of sensor nodes were (58 mm x 50 mm x 21 mm) and the data aggregation station (146 mm x 109 mm x 23 mm without antenna). Respected masses were: (42 grams) (each node) and (304 grams). Each node was instrumented with foil strain gauges in a full bridge configuration and a

temperature sensor (available inside LXRS® node). Wireless nodes were bolted to aluminum plate or secured inside special pockets on the ribbon as depicted in Figure 3. The figure also shows wiring of foil strain gauges. Over four hours of data were collected during the balloon flight. Strains and temperatures were measured every 3 milliseconds.

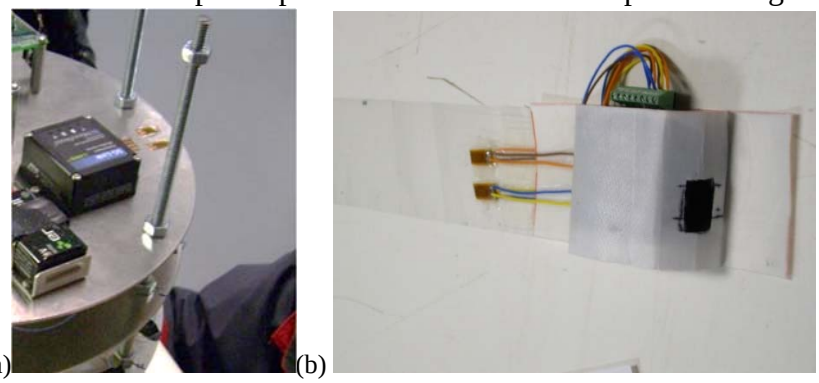

(a) (b)

Figure 3 SG-Link-LXRS wireless sensor node (a) inside payload (b) inside a special pocket on Mylar ribbon.

3.3 Active and passive embedded ultrasonic tests

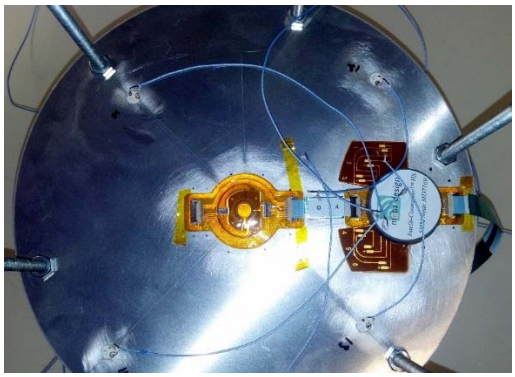

Figure 4 Signal generation and reception unit and transmitting and receiving sensors on an aluminum plate inside payload.

The university team collaborated with Metis Design Corporation on embedded ultrasonic tests. Signal generation, reception and processing were achieved using commercially available MD7 Digital SHM system (Figure 4) guided by broad durability studies [4]. The sensors utilized in this study were typical PZT (APC-851 piezoelectric ceramic disk with 7 mm diameter and 0.25 mm thickness) with a feedback electrode for one-side access. A special adaptor was necessary to facilitate use of these sensor with Metis hardware as it generally accepts special sensor layouts produced by Metis. Piezoelectric sensors were installed on aluminum plated using space-graded Hysol EA 9309 two part epoxy adhesive. Figure 5 depicts layout of embedded ultrasonic tests.

During stratospheric flight, the Metis hardware cycled between two different modes; the active and passive SHM. In the active mode, an ultrasonic pulse transmitted at frequencies ranging from 50 kHz to 500 kHz with 25 kHz increments. The configuration of receiving sensors depicted in Figure 5 allowed for simultaneous measurements of structural sound speed in aluminum plate, detection of a crack in a pitch-catch mode and assessment of integrity of bolted joints when an elastic wave was transmitted from upper to lower plates. The passive SHM was implemented by setting hardware into a listening mode, which allowed for collection of acoustic emission (AE) data during flight. The system would process 5 passive events for every active frequency sweep. Collection of AE data was triggered by AE signal reaching a certain level and was carried out for 0.5 ms before and 1 ms after trigger. As a result of this setup, four embedded ultrasonic experiments were conducted during stratospheric flight – 3 active and 1 passive.

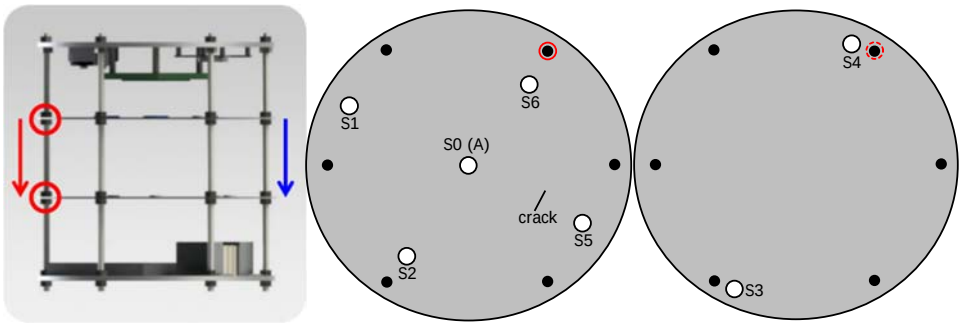

Figure 5 Sensor layout for embedded ultrasonic tests: schematics illustrating transmission through reduced torque (red) and healthy (blue) bolted joints, top plate with actuator in the center and receiving sensors, bottom plates showing receiving sensors for bolted joint assessment.

4. SHM RESULTS OF HIGH- ALTITUDE BALLOON FLIGHT

The balloon was launched on January 20, 2013 from a launch site near Madras, Oregon. Pre-launch procedures were completed at 9 am when power to all SMH experiments, except impedance measurements, were turned on. This time is labeled as "0" in Figure 6 and Figure 7 showing wireless strain and temperature data. Balloon preparation and release procedures follow during which a container housing the payload was opened and impedance measurement was turned on. Unfortunately, a flight delay has occurred and the balloon was released approximately one hour later resulting in impedance data collected on-the-ground only. Wireless sensor experiment and elastic wave propagation measurements were successfully conducted during the whole flight.

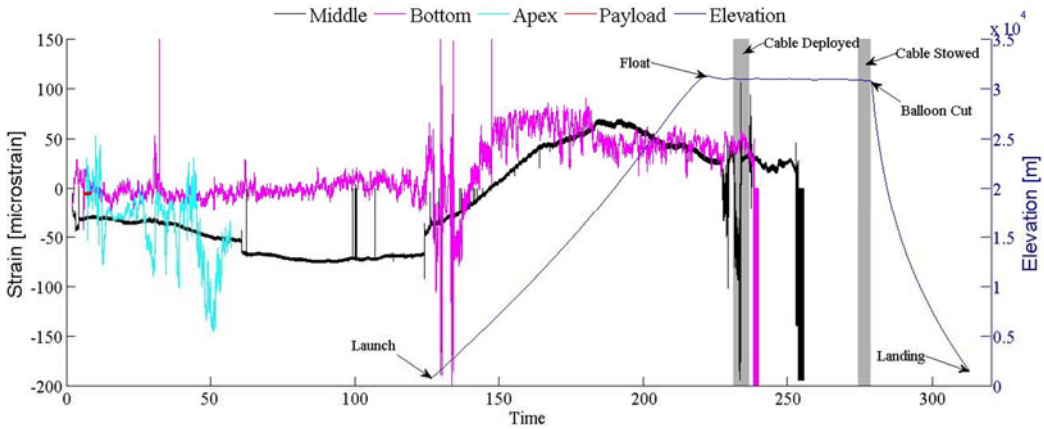

Figure 6 Strain data (left axis) collected wirelessly at elevations indicated on the right axis.

Figure 6 presents results of wireless strain measurements. Noticeable in the figure, payload and balloon apex nodes ceased transmission before launch. It has been postulated that the reason for transmission difficulties was opening and closing of the aluminum container housing the payload. The container enclosure created a unique RF environment which affected continuity of signal transmission. As anticipated, a node inside payload and in the middle of a ribbon in a pulley (protected by layers of Mylar tape) gave the most stable readings. Preparation of the balloon for launch was associated with substantial dynamics, which is reflected in apex node readings. The payload container experienced less structural disturbances with most dynamics seen by the node at the bottom of the Mylar ribbon (labeled cable), which was not secured but was hanging from a pulley. This node has shown considerable

dynamic events at launch and ribbon (cable) deployment. The middle node indicated dynamic event when a ribbon was deployed and signal inconsistencies right before data collection has stopped. It is suggested that wireless nodes stopped operating due to low temperatures as the nodes were qualified till -40 C^0.

Temperature data presented in Figure 7 indicates some temperature variability for sensors most exposed to environment. A temperature increase is noticeable as time changes from 9 am to 11 am. Instability in temperature readings is noticeable at the time of balloon launch and never stabilizes, which suggests some mechanical effect on sensor performance. A node at the middle of the ribbon collected adequate data when it was protected by layers of Mylar ribbon before the ribbon was deployed. Instability is noticeable at the time of ribbon deployment and the node stopped operation after temperature reached the lowest point (below - 40 C^0).

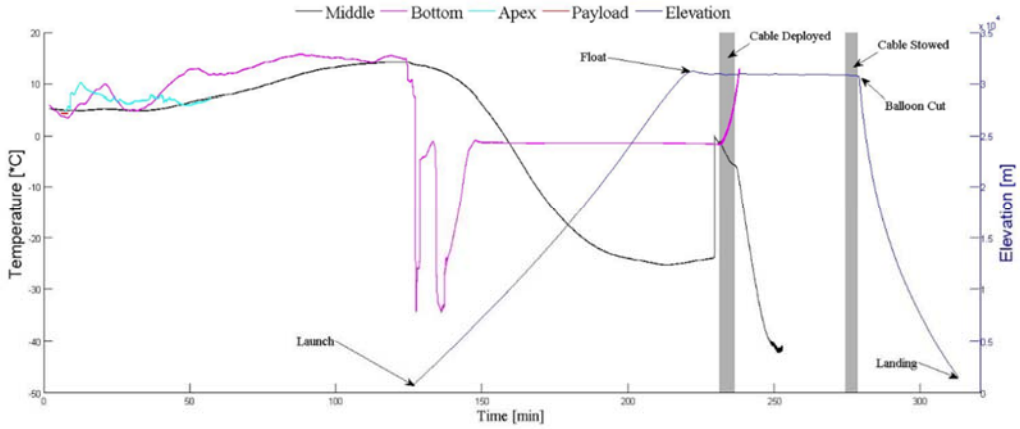

Figure 7 Temperature data (left axis) collected wirelessly at elevations indicated on the right axis.

Acoustic emission data was collected using passive data acquisition mode of the Metis Design MD7 Digital system. The data was collected before, during and after the flight for more than 8 hours of continuous data acquisition. To process such an enormous volume of data a special interface was written in Matlab®. Figure 8 illustrates an example of time and frequency domain AE data with distinctive features. Several interesting trends were uncovered with the most perplexing being periodic changes (7 minutes period) of distances between frequency peaks exemplified in the right part of Figure 8. Subsequent analysis indicated that the most vivid features seen in AE signal during the flight were related to electro-magnetic interference between electronic hardware components.

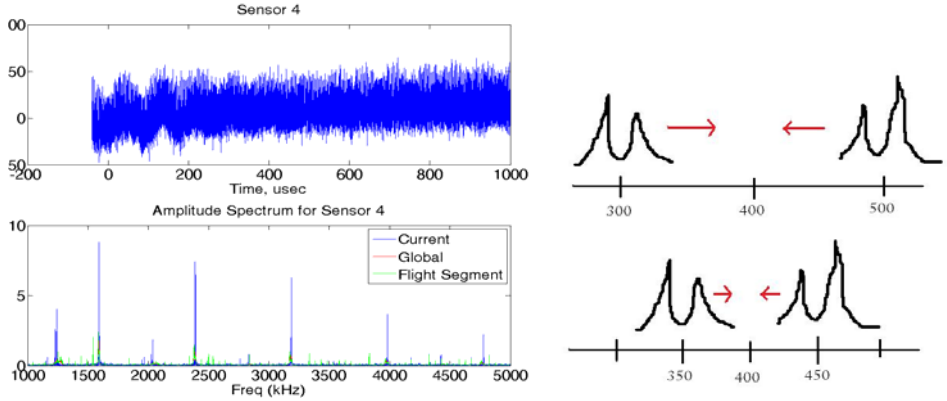

Figure 8 Example of acoustic emission data collected during flight.

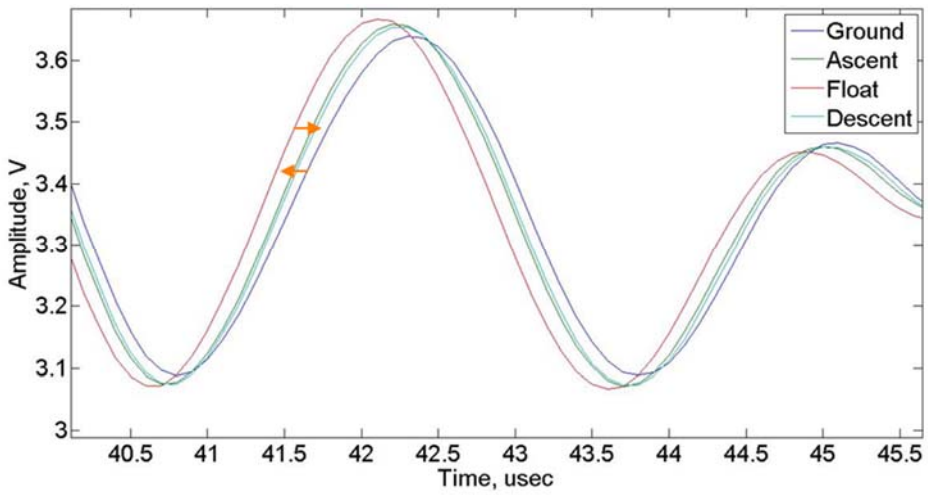

Figure 9 Elastic wave propagation data showing phase and amplitude changes for particular stages of stratospheric balloon flight.

The elastic wave propagation experiment demonstrated changes in structural sound speed at all stages of the stratospheric balloon flight. Example of the wave propagation data is presented in Figure 9 where phase and amplitude changes are clearly seen as the balloon stays on the ground, ascends, floats and descends. The data correlates with temperature profile of the mission as the wave shifts to the left at lower temperatures of the ascent stage, then again shifts left at very low temperatures of the float stage, and finally shifts right at warmer temperatures during payload descent.

Example of elastic wave data demonstrating feasibility of crack detection during stratospheric flight is presented in Figure 10a. In this experiment, a crack was imitated with a thin (1mm thick and 15mm long) slit in aluminum plate which was detected in a pitch-catch (through transmission) sensor setup. It can be seen from the figure that although crack detection is possible, environmental changes at all stages of stratospheric flight are more pronounced in the signals than changes due to crack.

Embedded ultrasonic detection of loose bolts [7] is also possible as suggested in Figure 10b. Elastic waves propagated through the loose bolted joint show considerably lower amplitude, higher signal nonlinearity and more pronounced influence of environmental factors affecting phase shifts of elastic waves.

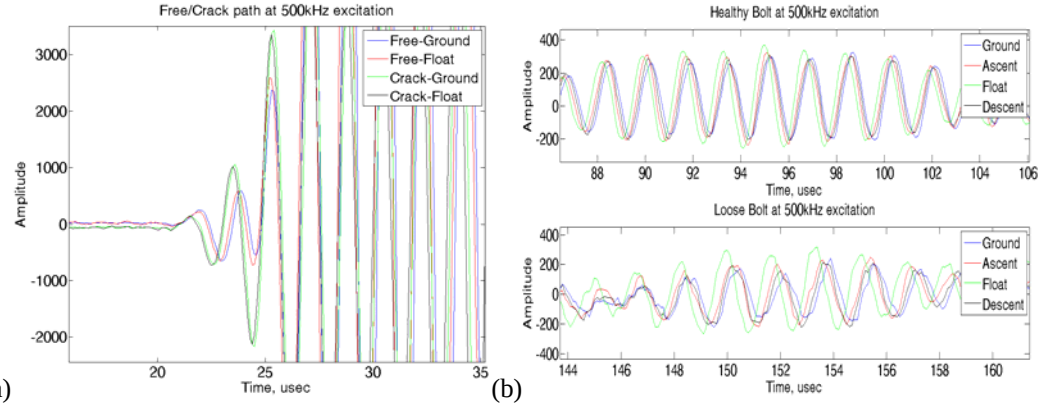

(a) (b)

Figure 10 (a) Pitch-catch detection of imitated crack, (b) detection of loose bolts.

5. CONCLUSION

In this contribution, SHM during high-altitude balloon flight is reported. Five

SHM experiments have been conducted showing feasibility of SHM in a near-space stratospheric environment. Strain and temperature data were collected wirelessly for several flight stages until sensor nodes stopped operating possibly due to very low temperatures. Strain data shows elements of payload and balloon dynamics and temperature data is consistent with observations. Acoustic emission data was masked with electromagnetic interference from electronic hardware components. Elastic wave propagation data correlates with temperature dependencies, which noticeably influence crack detection and integrity assessment of loose bolted joints. During the flight, successful detection of an imitated crack and loose bolted joints has been demonstrated.

6. ACKNOWLEDGMENTS

Authors would like to acknowledge undergraduate students who assisted in payload development, fabrication and launch: Joe MacGillivray, Sam Chesebrough, Levi Magnusion, Lloyd Puckett, Karen Tena, Jaclene Gutierrez, Blaine Trujillo, Tiffany Gonzales.

Nickolas Demidovich (FAA) is acknowledged for guidelines, expertise and rewarding discussions during payload development and launch.

The flight opportunity was provided by the NASA Flight Opportunities Program http://flightopportunities.nasa.gov , flight 38 BS.

Near Space Corporation (Tim Lachenmeier and the team) is acknowledged for payload integration, launch and recovery.

Federal Aviation Administration (FAA) through Center of Excellence for Commercial Space Transportation, AFRL Space Vehicles Directorate, and NMT Department of Mechanical Engineering are acknowledged for financial support.

Metis Design Corporation and LORD Microstrain are acknowledged for collaboration on measurement hardware and assistance with tests.

Los Alamos National Laboratory Engineering Institute is acknowledged for providing WID3 impedance measurements boards. Assistance of Charles Farrar, Stuart Taylor, and Gyuhae Park is appreciated.

7. REFERENCES

1. Champaigne, K (2005) "Wireless Sensor Systems for Near-term Space Shuttle Missions", International Modal Analysis Conference – IMAC 2005, Orlando, Florida, USA, 2005.
2. Baumann, E.W., Becker, R.S., Ellerbrock, P.J. and Jacobs, S.W. 1997. ‘‘DC-XA Structural Health Monitoring System,’’ Proceedings of SPIE’s Smart Structures and Materials, 3044:195206.
3. Trott, A. A. and Kevin Champaigne, K. B., “Wireless Sensors in Space – Three Families of Wireless Capability,” ETTC 2005 – European Test & Telemetry Conference.
4. Chambers J.T., Wardle B.L. and S.S. Kessler. "Lessons Learned from a Broad Durability Study of an Aerospace SHM System." Proceedings of the 6th International Workshop on Structural Health Monitoring, 11-14 September 2007, Stanford University.
5. Overly, T. G. S., Park, G., Farinholt, K. M. and Farrar, C. R. (2008) “Development of an extremely compact impedance-based wireless sensing device,” Smart Mater. Struct. 17 (2008) 065011 (9pp) doi:10.1088/0964-1726/17/6/065011.
6. http://institute.lanl.gov/ei/
7. Doyle, D., Zagrai, A., Arritt, B., Çakan, H., (2010) “Damage Detection in Bolted Space Structures,” *Journal of Intelligent Material Systems and Structures*, Vol. 21, N. 3, pp. 251-264, first published on November 25, 2009.